RSC Advances

ROYAL SOCIETY OF CHEMISTRY

www.rsc.org/advances

Micelles-templated synthesis of Pt hollow nanospheres for catalytic hydrogen evolution

Manickam Sasidharan,[a] *Piyali Bhanja,*[b] *Senthil Chenrayan*[a] *and Asim Bhaumik*[b]

[a] *SRM Research Institute, SRM University, Kattankulathur, Chennai, 603203, India, E-mail: sasidharan.m@res.srmuniv.ac.in*

[b] *Department of Material Science, Indian Association for the Cultivation of Science, Jadavpur, Kolkata 700 032, India, E-mail: msab@iacs.res.in.*

An alternate to Galvanic replacement reactions and hard-template strategies, we report an efficient, a mild and simple synthesis strategy for fabrication of colloidal hollow platinum (Pt) hollow nanospheres. An aqueous asymmetric triblock copolymer poly(styrene–*b*–vinyl-2-pyridine–*b*–ethylene oxide) [PS(20.1k)–PVP(14.2k)–PEO(26.0)] micelle with *core–shell–corona* architecture have been found to an efficient soft scaffold for the synthesis of Pt hollow nanospheres using K_2PtCl_6 as metal precursor and $NaBH_4$ as a reducing agent. In the *core–shell–corona* type micelles, the *core* serves as template for void volume creation, shell domain acts reaction site for inorganic precursors, and *corona* stabilizes the composite particles. The polymer/Pt composite particles were solvent-extracted by refluxing with dimethyl formamide (DMF) at 160 °C to remove polymeric materials and obtain hollow particles. Investigation of precursor concentrations suggested that the wall-structures become irregular and uneven as the molar ratios of PVP/Pt (IV) increases from 1 : 12 to 1 : 25. Whereas use of polymers with large PS block length [PS(45k)–PVP(16k)–PEO(8.5)] results in the formation of spherical particles with slightly increased hollow void-space diameters. The polymeric micelles and Pt hollow nanospheres were thoroughly characterized by transmission electron microscope (TEM), X-ray diffraction (XRD), infra-red (FT IR), thermal (TG/DTA) and nitrogen sorption

analyses. The catalytic activity of Pt hollow nanospheres was investigated for hydrogen liberation from ammonia-borane (AB) by hydrolysis reaction at room temperature. The catalytic activity of Pt hollow nanospheres reveals that it can serve as a promising heterogeneous catalyst towards hydrogen generation system using AB as solid hydrogen storage materials.

Introduction

Considerable attention has been paid for synthesis of nanostructured platinum (Pt) with controlled size and shape.[1-3] Much effort has also been focused on the morphological and structural features of Pt nanostructures to produce Pt catalysts with high surface area to volume ratio and consequently large fraction of the metal atoms that are exposed at surfaces are accessible to reactant molecules, thereby available for catalysis.[4,5] A number of synthetic methods have been reported in the past for preparation of Pt nanoparticles in organic solvents[6-8] and in aqueous solutions.[9,10] For instance, reduction of potassium tetrachloroplatinate in aqueous solution with hydrogen produced Pt nanoparticles of different shapes like cubic, tetrahedral, and truncated octahedral with diameters ranging from 2 to 11 nm.[11] It is suggested that the formation of these nanostructures are thermodynamically favored due to minimization of surface energy of these shape-dependent nanoparticles and perhaps, free energy of the system as a whole play an important role during the process of nucleation and growth. In addition, dendritic growth of small Pt nanoparticles[12,13] and mesoporous monocrystalline Pt nanoparticles with uniform shapes and size have also been investigated.[14,15] Thus intense research has been devoted to the fabrication of dense Pt-metal nanoparticles with tailored properties in size, shape, and composition. Furthermore, the synthesis and characterization of nanoparticles were mainly carried out in presence of capping agents with suitable functional groups to prevent them from

agglomeration due to van der Walls forces.[16] Although the polymer-stabilized noble metal colloids have great potential applications, often they exhibit decreased catalytic activity.[17,18] Thus the polymer-stabilized Pt nanoparticles showed lower activity than the colloidal platinum in the sol state (nascent state), although its activity can be enhanced through removal by the oxidation of the protective polymer through the calcination process. Thus, the protective polymer or organic stabilizing agent on the metal colloid is not preferable for majority of catalytic applications. Therefore preparation of nanoparticles without any capping agents to obtain "unprotected colloids" would be ideal for catalytic application as these particles would have large number of low-coordinated surface atomic sites that are largely responsible for catalytic reactions.[19]

Hollow metal micro//nanostructures are of great interest in many emerging area of technology. In a large number of applications such as catalysis, cosmetics, drug delivery, photonics, and rechargeable batteries, the chemical make-up and distribution of matter within the individual particles play important roles in determining specific function. For instance, one can tune the void-space and wall-thickness in hollow particles to control drug-release kinetics, modulate refractive index, increase active area for catalytic applications, improve cyclic volume change during repeated charge/discharging processes in a rechargeable batteries etc. Furthermore, hollow metallic nanospheres exhibit catalytic activities different from their solid counter parts with the advantages of low density apart from saving of materials. Traditional approaches to fabricate hollow nanospheres have focused on various sacrificial hard-templates, including polystyrene spheres,[20] silica spheres,[21] stabilizing agents,[22] sacrificial template,[23] liquid droplets,[24] and micro emulsion droplets.[25] Bai et al. have reported galvanic replacement reactions (also called sacrificial-template) for preparation of Pt hollow spherical particles of

average diameter of 24 nm using cobalt (Co) nanoparticles as sacrificial templates and citrate as a capping agent.[26] The wall-thickness of reported Pt hollow nanospheres mainly consisted of ca. 2 nm Pt nanoparticles with uneven wall-thickness comprising of large-pores and surface roughness. The hollow nanoparticles can fulfil our requirement in catalysis in a way that it not only avoids the use of stabilizing agents but also thin-wall structures have a large number of exposed surface atoms for catalytic applications.

Recently, triblock copolymers with three different chemical entities (ABC type) with hydrophilic- and hydrophobic-parts have been extensively studied for fabrication of inorganic hollow nanospheres. When dissolved in appropriate solvents followed by dialysis against water, these ABC type triblock copolymers forms *core–shell–corona* (CSC) type micelle which was efficiently used for construction of a variety of metal oxide, metal borate, silica, phosphosilicate and periodic mesoporous silica hollow nanospheres by self-assembly process in our group.[27-32] The notable features of ABC type triblock copolymers is that when dissolved in an appropriate solvent, it forms CSC micelles having both hydrophilic and hydrophobic characters and self-assemble in such a way that the hydrophobic *core* part acts as a template for void formation, the central hydrophilic *shell* domain serves as reaction site for reaction of inorganic metal precursors, and the hydrophilic *corona* block stabilizes the composite micelles. Herein we report a facile, efficient method for the synthesis of Pt hollow nanoparticles of average size 27± 2 nm templated by micelles of poly(styrene-*b*-vinyl-2-pyridine-*b*-ethylene oxide) (PS-PVP-PEO) using K_2PtCl_6 as metal source and sodium borohydride ($NaBH_4$) as a reducing agent under ambient reaction conditions. Thus obtained Pt hollow nanoparticles were thoroughly

characterized by XRD, TEM, FTIR, TG/DTA, DLS, and nitrogen sorption analyses to confirm the morphology, crystallinity and phase purity.

Hydrogen is one of the most promising energy carriers and is expected to replace fossil fuels as the dominating energy source in the future due to carbon-free cycle. However, finding efficient hydrogen generation materials is one of the bottlenecks for using hydrogen energy. Recently, ammonia-borane (H_3NBH_3, AB) has attracted much attention as an efficient H_2 storage materials due to its high hydrogen content (19.6 wt% H_2) and low molecular weight (30.7 g/mol).[33,34] AB is highly stable at room temperature and also readily soluble in water. Unlike borohydrides which require a base for stabilization, AB does not require any additional stabilizing agents and it releases hydrogen in the presence of a suitable catalyst.[35,36] A number of catalysts have been investigated for effective release of H_2 through hydrolysis of AB including various metal salts like $RuCl_3$, $PdCl_2$, and $CoCl_2$,[37] noble metal nanoclusters and non-noble metals supported on Al_2O_3, carbon and silica.[38,39] The efficacy of Pt hollow nanospheres in the hydrolysis of AB was determined by measuring the rate of hydrogen liberation using a jacketed round bottom flask with thermostat to control the temperature 25 ± 0.2 °C.

Experimental Section

Chemicals. Potassium hexachloroplatinate, (K_2PtCl_6, 99.9 %), sodium borohydride ($NaBH_4$, 99.0 %), ammonia-borane (H_3N-BH_3, 99.0 %), and N, N–dimethylformamide (DMF, 99.8 %) were obtained from Sigma–Aldrich and used as received. PS–PVP–PEO triblock copolymers with PS, PVP, and PEO having varying chain lengths ca. PS(20.1k)–PVP(14.2k)–PEO(26k) and PS(45k)–PVP(16k)–PEO(8.5k) were obtained from

Polymer Source Inc. The numbers in the parentheses are the average molecular weights of the block chains (20.1k, for example refer to 20100). Phosphotungstic acid hydrate ($P_2O_5.24WO_3.xH_2O$) and hydrochloric acid were obtained from SD fine chemicals. Water was purified with a Millipore Milli-Q water system.

Preparation of *core–shell–corona* micelles. A general procedure for preparation of PS–PVP–PEO micelles involves dissolution of desired amount (0.1 g) of PS(20.1k)–PVP(14.2k)–PEO(26k) in DMF containing 10 wt % water by stirring with a magnetic stirrer. The solvent DMF was removed through dialysis against water to obtain micelles of PS–PVP–PEO. The resultant solution was transferred to a 100 mL volumetric standard flask and diluted with Millipore water to obtain a polymer micelles concentration of 1.0 gL^{-1}. The micelle solution was adjusted to pH 4 with a dilute HCl solution which is used for fabrication of Pt hollow nanospheres. Whereas the micelle of (45k)–PVP(16k)–PEO(8.5k) was prepared according to report of Zhang and Eisenberg for "crew–cut" micelles[40] due to the reason that the water soluble hydrophilic PEO chain is much shorter than the hydrophobic PS chains. Therefore, (45k)–PVP(16k)–PEO(8.5k) was dissolved in DMF at the initial concentration of 1 wt%. After complete dissolution of polymer, water was added drop wise (1 wt% per minute) to the solution with vigorous stirring until the water content reached 5 wt%. The solution was then dialyzed as described above and the pH was also adjusted to 4 prior to synthesis of Pt hollow nanospheres.

Synthesis of Pt hollow nanospheres. In a typical synthesis of Pt hollow nanospheres using PS–PVP–PEO micelles (1.0 gL^{-1}) by $NaBH_4$ reduction is as follows. For example, 10 mL of above micelle solution was taken in round bottom flask. The pH was adjusted to about 4 using dil. HCl and the micelle solution was vigorously stirred at room temperature. The micelle

solution was initially purged with nitrogen gas to evacuate the air inside the vessel to remove the moisture inside the reaction vessel and then desired amount of K_2PtCl_6 (PVP/Pt = 12) was added. Subsequently, a dilute solution of $NaBH_4$ was added under N_2 flow and color of the solution changed from pale yellow to dark gray. The polymer/Pt composite particles were aged by stirring at room temperature for 48 h and separated by centrifugation (10000 rpm, 10 min). The solid was repeatedly washed with Milli-Q water and ethanol followed by drying at 50 °C. Similarly, other Pt hollow particles were carried by changing the molar ratio of Pt/PVP like 12, 18, and 25 under identical experimental conditions. Finally, the polymer/Pt composite particles were solvent extracted by refluxing in a DMF solvent using a reflux condenser at 160 °C for 8 h. After drying in a high vacuum pump, the obtained Pt hollow nanospheres without any stabilizing agents were stored in an argon atomosphere in a glove box to prevent the oxidation of Pt-surface due to moisture.

Characterization of materials. The hydrodynamic diameter (D_h) of polymeric micelles was measured with Zetasizer Nano of Malvern Instruments. The correlation functions were analyzed by the cumulant method to determine the diffusion coefficient (*D)* of the micelles. The hydrodymamic diameter (D_h) was calculated from D using the Stokes-Einstein equation: $D_h = k_BT/3\pi\eta D$, where k_B is the Boltzmann constant, T the absolute temperature, and η the solvent viscosity. Powder X-ray diffraction (XRD) pattern was measured on a Rigaku RINT-2200 diffractometer with CuKα radiation (40kV, 30 mA) from 10 ° to 70 ° 2θ in 0.01 steps at a scan speed of 2°/min. BET surface area was measured by N_2 adsorption/desorption analysis at 77 K on a BELSORB 28SA analyzer after degassing of the sample at 150 °C for 3 h. The TEM images were recorded on a JEOL Electron Microscope operationg at 80 kV and 200 kV. In the case of

micelle solutions, the TEM samples were prepared by casting a drop of micelle solution on a copper grid followed by staining with 1 wt% phosphotungstic acid, whereas for Pt nanospheres, a drop of aqueous suspension of the sample was coated on a copper grid. The samples were finally dried at room temperature. Thermogravimetric and differential thermograms (TG/DTA) were obtained with MAC Science TG-DTA 2100 under nitrogen. Fourier transform infrared (FTIR) spectra were recorded on Perkin Elmer spectrometer using KBr pellet technique. UV-visible spectra of gold nanoparticles were recorded with JASCO V-550 spectrometer using $BaSO_4$ as a reference.

Generation of hydrogen from ammonia-borane. The catalytic efficiency of Pt hollow nanospheres in the hydrolysis of ammonia-borane (AB) was determined by measuring the rate of hydrogen release at room temperature. In a typical reaction, 100 mL round bottom flask was mounted on a thermostat with temperature of 25 ± 0.2 °C by circulating water through its jacket from a constant temperature bath supplied by Heidolph, Germany. Then a graduated glass U-tube (100 cm in height and 36 mm in diameter) partially filled with water is connected to reaction flask through connectors and tubing's without any gas leak. AB (190.8 mg, 6 mmol) was dissolved in 30 mL water (Milli-Q) that corresponds to 18 mmol H_2 at 25 $^{\circ}$C and this solution was carefully transferred to the reaction flask with Teflon coated magnetic stirrer followed by addition of 1.91 mg of Pt hollow nanospheres (1 wt% with respect to AB) catalyst. The reaction was commenced immediately after the addition of catalysts to the magnetically stirred AB by closing the flask and the volume of hydrogen gas evolved was measured by recording the displacement of water level in U-tube.

Results and Discussion

The stepwise fabrication of Pt hollow nanospheres using *core–shell–corona* micelles of PS(20.1k)–PVP(14.2k)–PEO(26k) at pH 4 is depicted in Scheme 1. Prior to synthesis, the polymeric micelles were characterized for their structure and morphology by DLS and TEM. The TEM sample preparation was carried out by casting a drop of above micelle on a copper grid followed by staining with 1 wt% phosphotunsgtic acid and finally the grid was dried at room temperature. Figure 1 exhibits spherical micelles in which PVP shell domain was stained with phosphotungstic acid. The average micelle particle size was found to be 40 ± 2 nm with PS core having diameter of 22 ± 1 nm, whereas the estimated PVP shell thickness was 8 ± 0.5 nm. However, the average hydrodynamic diameters (D_h) of the above micelle estimated by dynamic light scattering experiments was found to be 64 nm. The smaller size observed (40 ± 2 nm) in TEM is due to exclusion of *corona* part and accounts only *core–shell* parts. At pH 4, the PVP shell of the PS–PVP–PEO micelles, in particular, PVP shell domain attains extended/stretched configuration due to repulsive forces among positively charged PVP units.[41-43] These features of PS–PVP–PEO micelles are utilized in the current investigation to prepare Pt hollow nanospheres under mild conditions.

On addition of K_2PtCl_4 solution, the polyvinyl-2-pyridine (PVP) blocks with positive charges electro-statically interacts with $PtCl_6^{2-}$ to give organic/inorganic composite particles as shown in the Figure 1B. The average size of composite particles was 47 ± 2 nm which is lower than the original micelle size estimated by DLS (64 nm). The $PtCl_6^{2-}$ species were reduced with $NaBH_4$ (molar ratio of $NaBH_4$/ K_2PtCl_4 = 3) at room temperature and the color of the solution

turned slowly in to dark gray. The formation of Pt nanoparticles is clearly seen by drawing a small aliquots of sample and analyzing through UV-visible spectra after 30 minutes (ESI. Fig. S1†). Fig.S1.A shows surface Plasmon resonance (SPR) bands at 522 nm corresponding to Pt-nanoparticles; whereas the band around 319 nm is ascribed to the presence of Pt(IV) ions in the reaction mixture.[44] In addition, the FTIR spectrum of composite particles (ESI. Fig.S2.A) shows a strong signal at 1720 cm^{-1} and a weak signal around 2913 cm^{-1} suggesting the presence of N–H stretching mode of PVP units; whereas the band at 1405 cm^{-1} is attributed to –C=C– bond stretching of phenyl groups of the polymer backbone. Absorption involving C–H bonds is found at 1182 cm^{-1} (in-plane bending modes) and 821 cm^{-1} (C–H wagging modes).[45] The TG/DTA analyses (ESI. Fig.S3†) indicated a complete decomposition of polymeric template at about 300 °C; however, in the current strategy, the polymer was freed from the composite particles through solvent extraction by refluxing with DMF for 8 h and is repeated thrice to ensure the complete removal. The FTIR spectrum (ESI, Fig.S2.B†) shows complete removal of organic polymers from absence of characteristic absorption bands. Furthermore after solvent extraction, the UV-visible spectra showed exclusively single band located at about 522 nm suggesting that all Pt(IV) ions were reduced to Pt(0) (ESI, Fig. S1.B†).

Fig.2 TEM(A-C) micrographs show Pt hollow nanospheres in the absence of any stabilizing agents having different shell-thickness obtained by varying the molar ratio of K_2PtCl_6/PVP 12, 18, and 25. The specific attributes of Pt hollow nanospheres such as particle's diameter, hollow void size, and wall-thickness were estimated from the TEM image. For instance, Pt hollow particles synthesized with a molar ratio of K_2PtCl_6/PVP = 12 (Fig.2.A) showed an average particle size of 26 ± 2 nm with wall thickness of about 5.5 ± 0.5 nm and

hollow void-space diameter was found to be 15 ± 0.5 nm. Almost all the hollow particles show a uniform spherical shape with a smooth shell wall. It is seen from TEM image that, similar to coalescing of other nanoscale materials due to their very high surface area to volume ratio vis-à-vis surface free energy, the Pt hollow particles also exhibit aggregation inherent to particle size in the absence of any stabilizing agents. It is also worth to mention that the wall-structure is completely formed without any breakage unlike hollow particles obtained by Galvanic replacement reactions or hard-template strategies. For instances, the hollow particles obtained by Galvanic replacement reactions using cobalt-nanoparticles template showed high degree of non-uniformity in the wall-structure as well as void-volumes and also surface is very rough.[27] Even the hard-template approach using silica spherical particles also yielded hollow nanospheres with irregular shell-thickness, void-space, and particle-size.[45] The significant development of this approach compared to previous strategies is that the shell-thickness increases to certain extent by increasing the amount of K_2PtCl_6. Fig. 2B and 2C shows TEM pictures of Pt hollow nanospheres obtained by varying the molar ratio of K_2PtCl_6/PVP = 18 and 25, respectively. Thus, as the metal precursor concentration increased from 18 to 25, the shell-thickness increased to 9.5 ± 0.5 nm (average particle size and void volumes were 29 ± 2 nm and 12 ± 1 nm, respectively) from 7.0 ± 0.5 nm. It is also commonly noticed that at K_2PtCl_6/PVP = 25, the hollow particles are rather not uniform and has broad size distribution which ranges from 22 nm to 34 nm due to deposition of a large amount of metal precursors in the *shell* domain of the micelles. Furthermore two or more micelles may have combined to form large hollow particles as seen from Fig.2C. It is also expected that the variation in the chain length of hydrophobic PS block of the template copolymer would be expected to increase the void space diameter.[46]

As the molecular weight of the PS block is increased from 20.1k to 45k, the hollow void space diameter expected to enlarge because the PS block serves as the template for void space formation. Fig. 3A shows TEM micrographs with increased void volume synthesized using polymer PS(45k)–PVP(16k)–PEO(8.5k) with higher PS molecular weight. The average particle size was found to 29 ± 2 nm having wall thickness of 5 ± 0.5 nm, whereas the estimated void-volume is 19 ± 0.5 nm. Therefore comparison of Figures 2A and 3A, it is evident the void space diameter of Pt-hollow particles can be increased over few nanometers by changing the PS block length. Fig. 3B exhibits high-resolution TEM (HRTEM) indicating lattice fringes originating from a Pt hollow nanoparticles and the lattice spacing of 0.235 nm corresponding to (111) plane for fcc Pt.[13] The electron diffraction (ED) pattern of Pt nanoparticles also clearly shows the presence of (111), (200), and (220) diffractions (Fig.3C) confirming phase pure Pt nanoparticles. The powder XRD pattern of Pt hollow nanospheres were recorded both prior to and after solvent extraction with DMF in the range of 30 – 70° 2θ (Fig.4). Both samples exhibited diffraction pattern peaks corresponding to (111), (200), and (220) planes similar to electron diffraction confirming the crystallinity and phase purity of Pt hollow nanospheres. BET surface area was found to be 36 m^2g^{-1} as estimated by nitrogen adsorption/desorption analyses (ESI, Fig.S4) of Pt hollow nanoparticles under liquid-nitrogen temperature (77 K). The above characterized Pt hollow nanospheres were investigated for generation of hydrogen through hydrolysis of ammonia-borane (AB) at 25 °C.

Nanoparticles of Pt with different shape and size were tested as catalyst in the hydrolysis of AB and the hydrogen liberation depends on the composition and distribution of Pt within the nano-structures. The dependence of the catalytic activity of Pt nanoparticles was investigated

with different Pt loading using Pt hollow nanospheres with wall-thickness of 5.5 ± 0.5 nm (obtained from Pt(IV)/PVP = 12) as standard catalysts. Fig.5 shows the variation in the catalytic activity of Pt nanoparticles with Pt loading in the hydrolysis of AB under identical experimental conditions with initial concentration of 6 mmol of AB. As the percentage of catalyst loading increases, the evolution of hydrogen was observed at faster rate compared to lower loadings. The observed catalytic activity could be explained by the availability of a large number of nanoparticles with huge number of active sites or binding sites at high Pt loadings. Furthermore, we also tested for any traces of ammonia formation during the hydrolysis of AB using acid/base indicator and showed no detectable amount of ammonia under the experimental conditions. In addition, to acquire meaningful catalytic data the hydrolysis of AB was carried out at lower conversion rate using 1 % Pt hollow nanospheres (controlling experiments at high Pt loading also rather difficult due fast evolution of hydrogen) for further investigation. Fig.6 exhibits the plots of the volume of generated hydrogen versus time over 1 % Pt hollow nanospheres (wall-thickness of 5.5 ± 0.5 nm, Pt(IV)/PVP = 12) at temperatures ranging from 25–40 °C starting with initial AB concentration of 6 mM. As expected, the volume of liberated hydrogen increases monotonically as the temperature increases from 25 ° to 40 °C and lead to near complete conversion of AB in a short duration (less than 30 minutes). It is well known that the reaction rate generally increases with rise of reaction temperature. The AB concentration decreases with reaction time and volume of H_2 generated increases nearly linearly with time. Under our experimental conditions, the reaction rate constant, k, is nearly constant for a given temperature, implying zero order kinetics for the AB hydrolysis reaction as observed by other researchers.[39] Thus using the rate law $-1/3\ d[NH_3BH_3]/dt = d[H_2]/dt = k$ and rate equation $k = \exp^{-E/RT}$, where E is activation energy, R the gas constant, and T is the reaction temperature.[39] The Arrhenius

plots obtained from log k versus the reciprocal absolute temperature (ESI. Fig.S5†) and the estimated activation energy from the slope of straight line was found to be 22.7 kJ mol^{-1} which is comparable to the literature reports.[38,39] To maintain the controlled release of hydrogen at room temperature, the subsequent studies were carried out at 25 °C using 1 wt% Pt hollow nanospheres.

Fig.7 exhibits catalytic activities of Pt nanoparticles with different morphological features such as hollow nanospheres, dense spheres, and ligand-stabilized nanoparticles of size similar wall-thickness of hollow nanospheres. Among the various particles tested for hydrolysis of AB, Pt hollow nanospheres with wall-thickness of 5.5 nm showed highest activity under similar experimental conditions; however, hollow nanoparticles with wall thickness of 9.5 nm also realized nearly similar activity and no significant difference was observed. This observed results suggest that no appreciable difference in the catalytic activity was noticed when the shell-thickness of hollow particles decreases below 10 nm. It is important to mention that Pt hollow nanospheres of size about 1–2 μm showed less activity than the bimetallic clusters[47] and it can be accounted based nano-size effects. As the particle sizes are reduced from micrometer to nanometer range, the surface area vis-à-vis binding sites of catalysts increases proportionally and hence show enhanced catalytic activity compared to their corresponding micron sized particles. More interestingly, the ligand-stabilized Pt nanoparticles of size approximately 5–10 nm (ESI. Fig.S6†) shows appreciably less activity which could be due to the following reason. In the case of functionalized or stabilized nanoparticles, the stabilizing agents always encapsulates or binds with the metal surface to reduce surface free energy vis-à-vis number of binding sites available for catalysis and hence it shows lower catalytic activity than the unmasked hollow nanospheres

having shell thickness of 5–10 nm under investigation. We have also studied dense spherical Pt particles of size 30–40 nm (ESI. Fig. S7†). It exhibited lowest activity among the various catalysts investigated in this study and the decreased activity might be due to direct consequence of less number of binding sites available for catalysis. Obviously the thin-wall structures (5–10 nm) of hollow nanospheres could efficiently promote catalytic reactions and effectively circumvent the adverse effects of masking agents in the liberation of hydrogen. After hydrolysis of AB, the catalyst was isolated by suction filtration and dried under nitrogen atmosphere. The isolated catalysts are reused again and studied for reusability test. We have reused the same Pt nanocatalyst successively for five times and negligible loss of catalytic activity was noticed (ESI. Fig.S8†). The minor decrease in catalytic conversion of AB in subsequent runs may be due to the material loss during isolation or due to passivation of Pt hollow nanospheres surface by increasing amount of metaborate (byproduct), which might decrease the accessibility of active sites.[48,49] Furthermore, it is worth to point out the Pt-hollow nanospherical particles mostly retained their spherical morphology as shown in Fig.S9 supporting information and aggregation occurs to a less extent. The above study suggests that Pt hollow nanospheres can be used as effective heterogeneous catalysts for liberation of hydrogen from AB under mild experimental conditions.

Conclusions

ABC triblock copolymers of type PS–PVP–PEO with *core–shell–corona* architectures can be effectively used as soft templates for fabrication Pt hollow nanospheres of size less than 30 nm under mild experimental conditions. The synthesis of Pt hollow nanospheres with different K_2PtCl_6/PVP mole ratios confirmed that the wall-thickness can be increased over several

nanometers. The use of triblock copolymers with different PS core block lengths such as PS(20.1k)–PVP(14.2k)–PEO(26k) and PS(45k)–PVP(16k)–PEO(8.5k) led to formation of hollow nanospheres with slightly increased void-space diameters. Investigation by FTIR spectroscopic study suggested that the solvent extraction using DMF effectively removes polymeric templates from composite particles to provide Pt hollow nanospheres. High resolution TEM, electron diffraction pattern, and X-ray diffraction results confirmed that the hollow spherical nature of Pt nanoparticles with very high crystallinity. The Pt hollow nanospheres serve as an efficient heterogeneous and reusable catalyst for hydrolysis of ammonia-borane under mild conditions. The hollow nanoparticles with wall-thickness of less than 10 nm exhibit very good activity in the liberation of hydrogen from AB compared to either dense Pt spherical particles of similar size or ligand-stabilized Pt nanoparticles of size less than 10 nm, suggesting potential application of Pt hollow nanospheres in hydrogen evolution reactions.

Acknowledgement

M. S. thanks Science & Engineering Research Board for their research support (No SB/S1/PC-043/2013). P. B. thanks CSIR, New Delhi for a junior research fellowship.

Supporting Informations

†Electronic Supplementary Information (ESI) available: [UV-visible, FTIR spectra, TG/DTA, nitrogen adsorption/desorption isotherm, TEM pictures Pt nanoparticles of different sizes and catalyst reusability data].

Notes and References

1 R. Narayanan and M. A. El-Sayed, *Nano Lett.* 2004, **4**, 1343–1348.

2 Y. Song, Y. Yang, C. J. Medforth, E. Pereira, A. K. Singh, H. Xu, Y. Jiang, C. J. Brinker, F. Swol and J. Shelnutt, *J. Am. Chem. Soc.* 2004, **126**, 635–645.

3 H. Wang, H. Y. Jeong, M. Imura, L. Wang, L. Radhakrishnan, N. Fujita, T. Castle, O. Terasaki and Y. Yamauchi, *J. Am. Chem. Soc.* 2011, **133**, 14526–14529.

4 B. Lim, X. M. Lu, M. J. Jiang, P. H. C. Camargo, E. C. Cho, E. P. Lee and Y. N. Xia, *Nano Lett.* 2008, **8**, 4043–4047.

5 J. Ren and R. D. Tilley, *J. Am. Chem. Soc*. 2007, **129**, 3287–3291.

6 C. Wang, H. Daimon, Y. Lee, J. Kim and S. Sun, *J. Am. Chem.Soc*. 2007, **129**, 6974–6975.

7 N. R. Jana and X. Peng, *J. Am. Chem. Soc*. 2003, **125**, 14280–14281.

8 M. Zhao and R. M. Crooks, *Adv. Mater*. 1999, **3**, 11-23.

9 Y. D. Liu, Z. Fang, L. Kuai and B. Y. Geng, *Nanoscale*, 2014, **6**, 9791-9797 .

10 K. Niesz, M. Grass and G. A. somorjai, *Nano Lett*. 2005, **5**, 2238–2240.

11 J. M. Petroski, T. C. Green and M. A. El-Sayed, *J. Phys. Chem. A* 2001**, 105**, 5542–5547.

12 M. A. Mahmoud, C. E. Tabor, M. A. El-Sayed, Y. Ding and Z. L. Wang, *J. Am. Chem. Soc.* 2008, **130**, 4590–4591..

13 L Wang and Y. Yamauchi, *J. Am. Chem. Soc*. 2009, **131**, 9152–9153.

14 Y. Yamauchi, A. Takai, T. Nagura, S. Inoue and K. Kuroda, *J. Am. Chem. Soc*. 2008, **130**, 5426–5427.

15 H. Wang, H. Y. Jeong, M. Imura, L. Wang, L. Radhakrishnan, N. Fujita, T. Castle, O. Teraski and Y. Yamauchi, *J. Am. Chem. Soc*. 2011, **133**, 14526-14529.

16 M. T. Reetz, W. Heibig and S. A. Quaiser, *Chem. Mater*. 1995, **7**, 2227–2228.

17 M. Ohtaki, M. Komiyama, H. Hirai and N. Toshima, *Macromolecules*, 1991, **24**, 5567−5572.

18 Q. Wang, H. Liu and H. Wang, *J. Colloid Interface Sci*. 1997, **190**, 380−386.

19 H. S. Taylor, *Proc. R. Soc. London Ser*. A 1925, **108**, 105

20 F. Caruso, R. A. Caruso and H. Möhwald, *Science*, 1998, **282**, 1111−1114.

21 21 S. W. Kim, M. Kim, W. Y. Lee and T. Hyeon, *J. Am. Chem. Soc.* 2002, **124**, 7642−7643.

22 S. Moreton, K. Faulds, N. C. Shand, M. A. Bedics, M. R. Detty and D. Graham, *Nanoscale*, 2015, **7**, 6075-6082.

23 H. T. Schmidt and A. E. Odtafin, *Adv. Mater.* 2002, **14**, 532−535.

24 T. Nakashima and N. Kimizuka, *J. Am. Chem. Soc*. 2003, **125**, 6386−6387.

25 S. Schacht, Q. Huo, I. G. Voigt-Martin, G. D. Stucky and F. Schuth, *Science* 1996, **273**, 768−771.

26 H-P. Liang, H-M. Zhang, J-S. Hu, Y-G. Guo, L-J Wan and C-L. Bai, *Angew. Chem. Int. Ed.* 2004, **43**, 1540−1543.

27 M. Sasidharan, K. Nakashima, Acc. Chem. Res. 47 (2014) 157-167.

28 M. Sasidharan, K. Nakashima, N. Gunawardhana, T. Yokoi, M. Inoue, S. Yusa, M. Yoshio, T. Tatsumi, Chem. Commun. 47 (2011) 6921-6923.

29 M. Sasidharan, N. Gunawardhana, M. Inoue, S. Yusa, M. Yoshio, K. Nakashima, Chem. Commun. 48 (2012) 3200-3202.

30 M. Sasidharan, H. Zenibana, M. Nandi, A. Bhaumik, K. Nakashima, Dalton Trans. 42 (2013) 13381-13389.

31 M. Sasidharan, K. Nakashima, N. Gunawardhana, T. Yokoi, M. Ito, M. Inoue, S. Yusa, M. Yoshio and T. Tatsumi, *NanoScale*, 2011, **3**, 4768-4773.

32 S. K. Das, M. K. Bhunia, D. Chakraborty, A. R. Khuda-Bukhsh and A. Bhaumik, *Chem. Commun*. 2012, **48**, 2891-2893.

33 B. Peng and J. Chen, *Energy Environ Sci.* 2008, **1**, 479−483.

34 T. Umegaki, J. M. Yan, X. B. Zhang, H. Shioyama, N. Kuriyama and Q. Xu, *Int. J Hydrogen Energy* 2008, **34** (5), 2303−2311.

35 T. U, Umegaki, J. M. Yan, X. B. Zhang, H. Shioyama, N. Kuriyama and Q. Xu, *Int. J Hydrogen Energy* 2009, **34** (9), 2303–2311.

36 P. V. Ramachandran and P. D. Gagare, *Inorg. Chem.* 2007, **46**, 7810–1817.

37 Q. Xu and M. Chandra, *J. Power Sources*, 2006, **163**, 364–370.

38 M. Chandra, Q. Xu, *J. Power Sources*, 2006, **163**, 855–861.

39 M. Chandra and Q. Xu, *J. Power Sources*, 2007, **168**, 135–142.

40 L. Zhang and A. Eisenberg, *Science* 1995, **268**, 1728–1731.

41 J. F. Gohy, N. Willet, S. Varshney, J. X. Zhang and R. Jerome, *Angew. Chem. Int. Ed.,* 2001, **40**, 3214–3216.

42 L. Lei, J. F. Gohy, N. Willet, J. X. Zhang, S. Varshney and R. Jerome, *Macromolecules*, 2004, **37**, 1089-1094.

43 M. Stepanek, J. Humpolickova, K. Prochazka, M. Hof, Z. Tuzar, M. Spirkova and T. Wolff, *Collect. Czech. Chem. Commun*, 2003, **68**, 2120–2138.

44 T. Herricks, J. Chen and Y. Xia, *Nano Lett*. 2004, **4**, 2367–2371.

45 H. Perez, J. P. Pradeau, P. A. Albouy and J. P. Omil, *Chem. Mater*. 1999, **11**, 3460–3463.

46 M. Sasidharan, D. Liu, N. Gunawardhana, M. Yoshio and K. Nakashima, *J. Mater. Chem.* 2011, **21**, 13881–13888.

47 Qin, C. Yang, X. Ma and S. Lai, *J. Alloys Compd.* 2011, **509**, 338–342.

48 T. J. Clark, G. R. Whittell and K Manners, *Inorg. Chem.* 2007, **46**, 7522–7527.

49 C. A. Jaska, T. Clark, S. B. Clendenning, D. Groeza, A. Turak and Z. H. Lu, *J. Am. Chem. Soc.* 2005, **127**, 5116–5124.

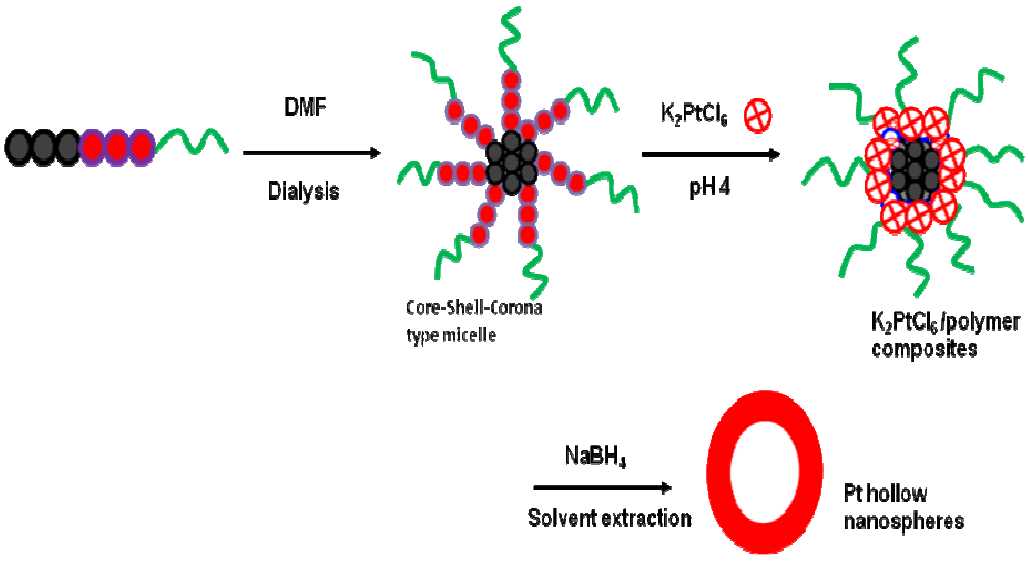

Scheme 1. Schematic representation of formation of Hollow nanosphere

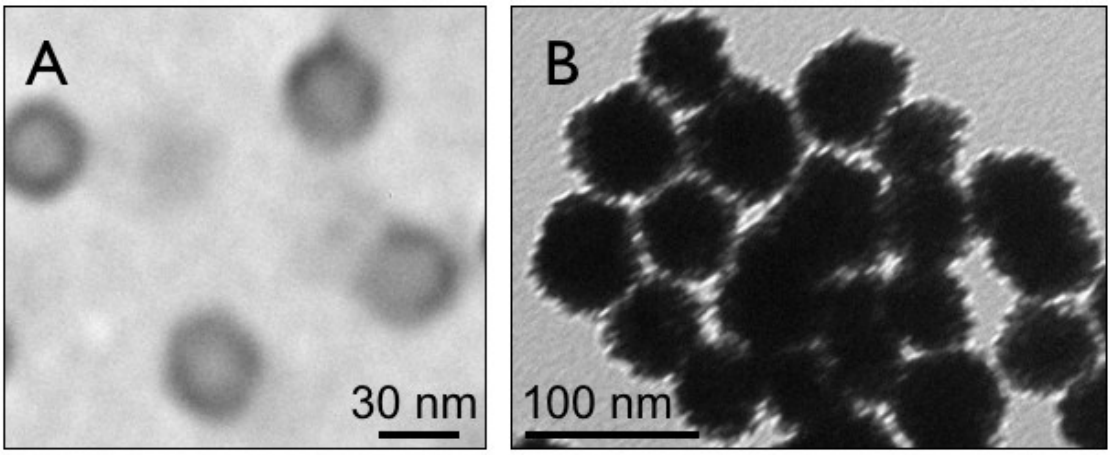

Figure 1. (A) TEM image of PS-PVP-PEO micelles and (B) Pt/polymer composite particles

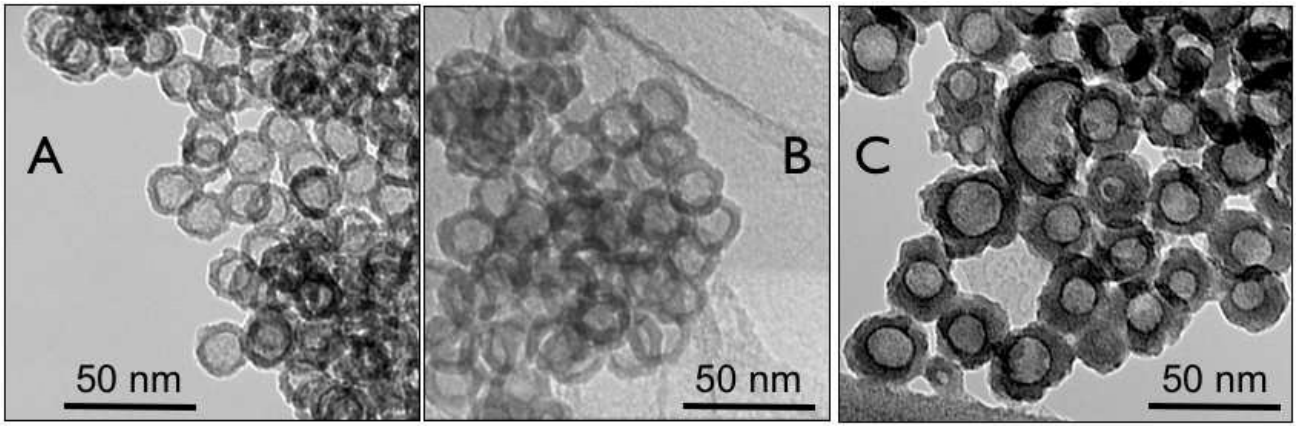

Figure 2. TEM images of Pt hollow nanospheres with varying precursors ratio; (A) K_2PtCl_6/PVP 12; (B) K_2PtCl_6/PVP 18; and (C) K_2PtCl_6/PVP 25

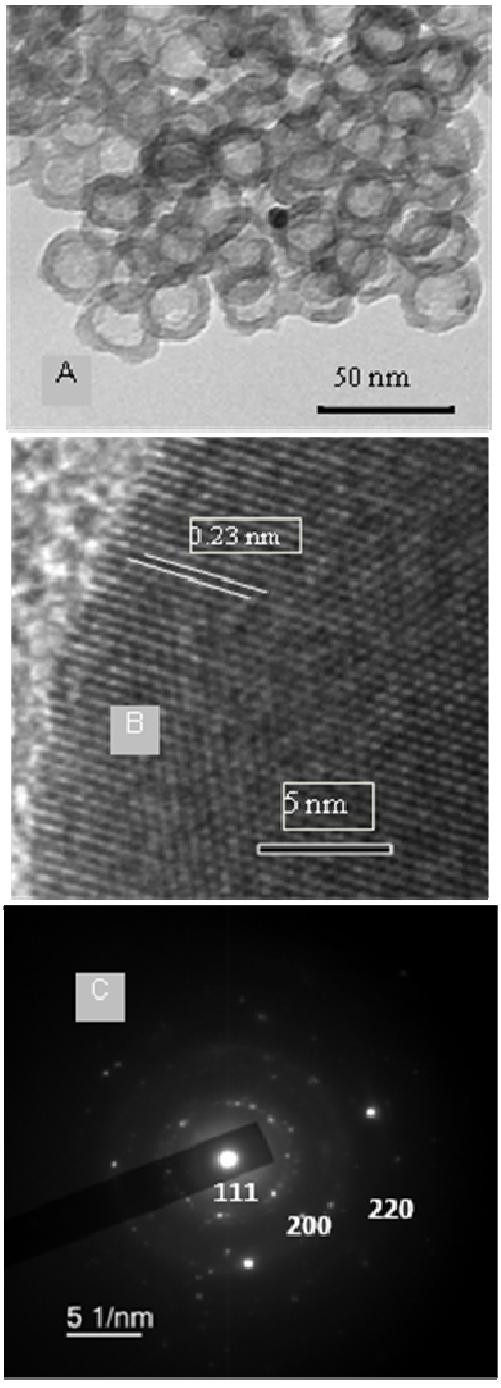

Figure 3. (A) TEM images of Pt hollow nanospheres with slightly increased void volume; (B) High resolution TEM of Pt hollow nanospheres; and (C) Electron diffraction pattern.

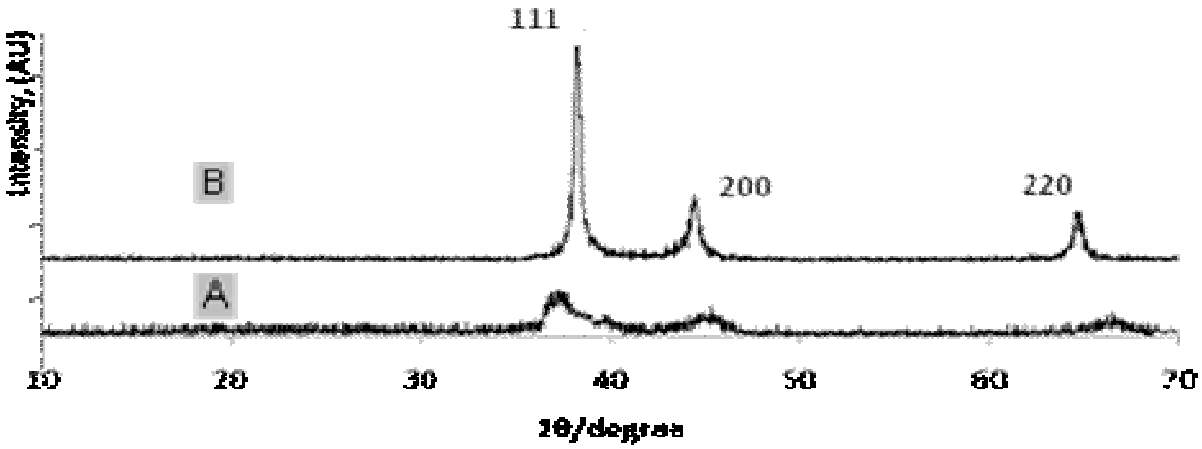

Figure 4. X-ray diffraction pattern of Pt hollow nanospheres; (A) Pt/polymer composite particles; and (B) solvent extracted Pt-hollow nanospheres.

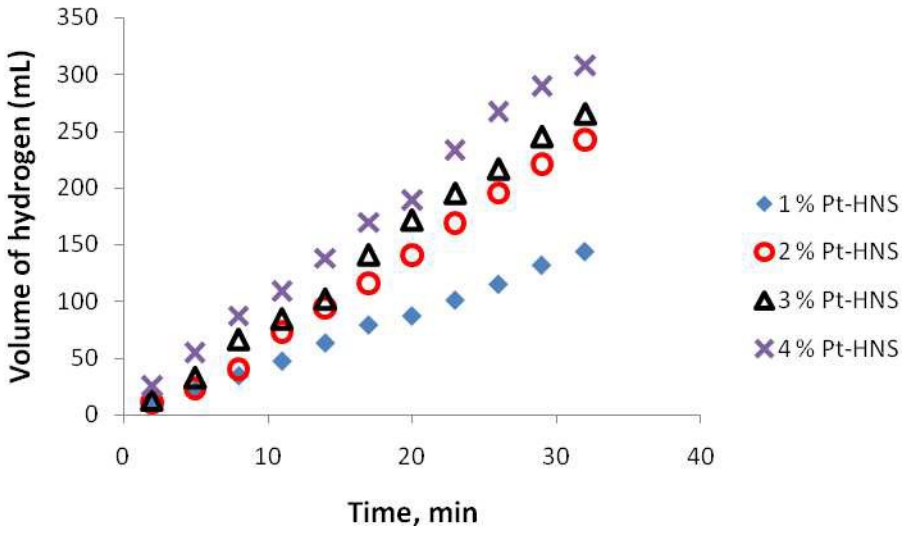

Figure 5. Effect of catalysts loading (Pt-hollow nanospheres) over the volume of generated hydrogen (mL) versus time for the hydrolysis of ammonia-borane.

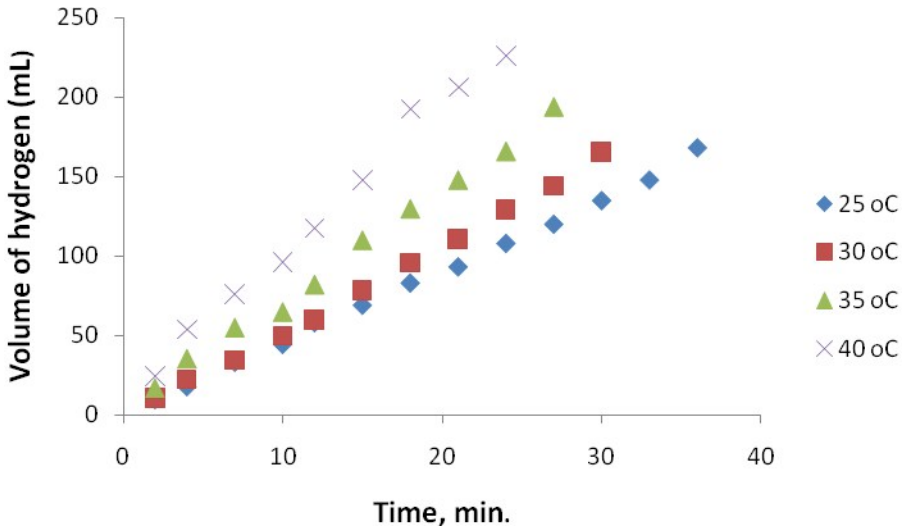

Figure 6. Effect of temperature (Pt-hollow nanospheres) over the volume of generated hydrogen (mL) versus time for the hydrolysis of ammonia-borane.

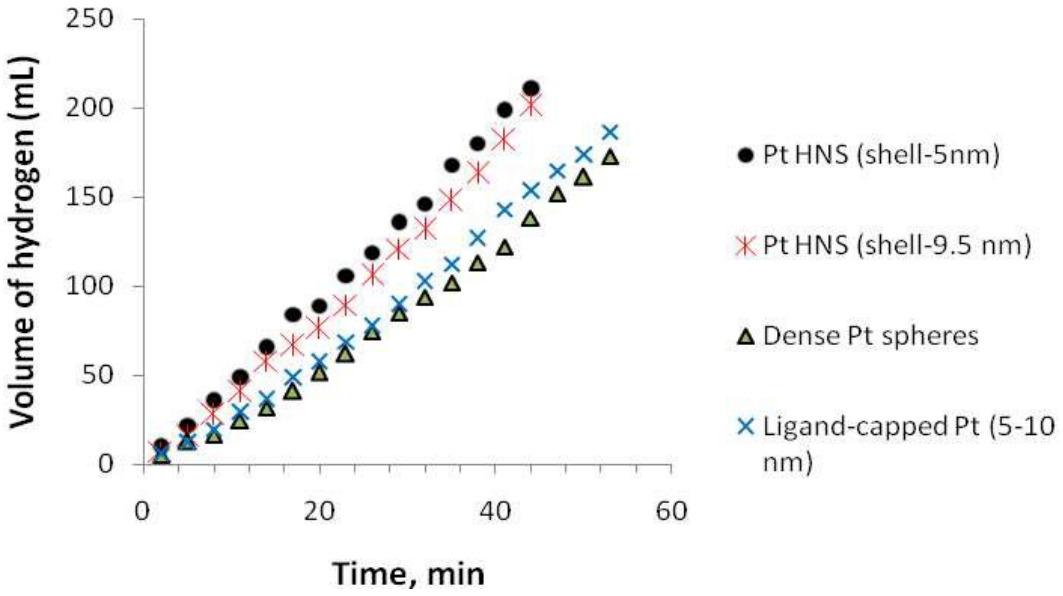

Figure 7. Effect of Pt-nanoparticles with different sizes (Pt-hollow nanospheres) over the volume of generated hydrogen (mL) versus time for the hydrolysis of ammonia-borane.

Table of Content

Micelles-templated synthesis of Pt hollow nanospheres for catalytic hydrogen evolution

Manickam Sasidharan, Piyali Bhanja, Senthil Chenrayan and Asim Bhaumik

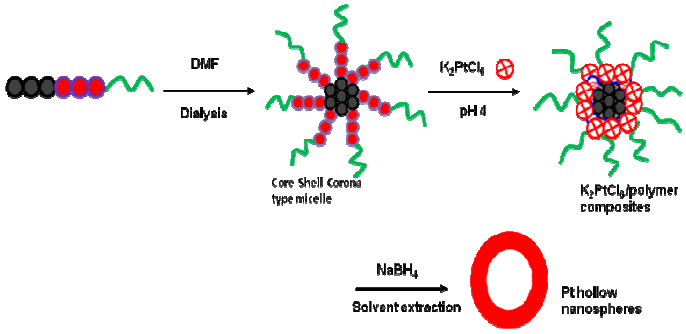

An alternate to Galvanic replacement reactions and hard-template strategies, we report an efficient, a mild and simple synthesis strategy for fabrication of colloidal hollow platinum (Pt) hollow nanospheres with ability to tune wall-thickness and void-space over several nanometers for catalytic application in evolution of hydrogen from ammonia-borane.